

The Sambungmacan 3 *Homo erectus* Calvaria: A Comparative Morphometric and Morphological Analysis

ERIC DELSON,^{1–4*} KATERINA HARVATI,^{1–4} DAVID REDDY,^{4,5}
LESLIE F. MARCUS,^{3,4,6} KENNETH MOWBRAY,^{7,8} G. J. SAWYER,⁷
TEUKU JACOB,⁹ AND SAMUEL MÁRQUEZ^{1,2,4,10}

¹Department of Anthropology, Lehman College/CUNY, New York

²Ph.D. Program in Anthropology, CUNY Graduate Center, New York

³Division of Paleontology, American Museum of Natural History, New York

⁴New York Consortium in Evolutionary Primatology, New York University, New York

⁵American Museum of Natural History, New York

⁶Department of Biology, Queens College/CUNY, New York

⁷Division of Anthropology, American Museum of Natural History, New York

⁸Department of Anthropology, Rutgers University, New Jersey

⁹Laboratory of Paleoanthropology, Gadjah Mada University, Yogyakarta, Indonesia

¹⁰Department of Cell Biology and Anatomy, Mount Sinai School of Medicine, New York

ABSTRACT

The Sambungmacan (Sm) 3 calvaria, discovered on Java in 1977, was illegally removed from Indonesia in 1998 and appeared in New York City in early 1999 at the Maxilla & Mandible, Ltd. natural history shop. Here we undertake an analysis of its phylogenetic and systematic position using geometric morphometrics and comparative morphology. The coordinates of points in the sagittal plane from glabella to opisthion were resampled to yield “lines” of 50 semi-landmarks. Coordinates of glabella, bregma, lambda, inion, and opisthion were also collected and analyzed separately. Casts of *Homo erectus* fossils from Indonesia, China, and Kenya and of “archaic *H. sapiens*” from Kabwe and Petralona, as well as 10 modern human crania, were used as the primary comparative sample. The modern humans were well separated from the fossils in a graphical superimposition of Procrustes-aligned semi-landmarks as well as in principal component and canonical discriminant analyses. In all of these, Sm 3 falls intermediate between the fossil and modern groups. Morphological comparisons of Sm 3 with a selection of *Homo erectus* fossils revealed its greatest similarity to specimens from Ngandong and the Sm 1 calvaria. Compared to all other *H. erectus*, Sm 3 was distinctive in its more vertical supratotal plane, less anteriorly projecting glabella and less sharply angled occiput. In these features it was somewhat similar to modern humans. It is not yet possible to determine if this similarity implies an evolutionary relationship or (more likely) individual or local population variation. Several features of Sm 3 (small size, gracile supraorbital torus and lack of angular torus, and position in principal component analysis) suggest that it was a female. The use of geometric morphometrics provides a means to statistically test the shapes of such fossils in a manner not easily duplicated by other methods. The intermediate position of Sm 3 between fossil and modern samples in several different subanalyses exemplifies the value of this approach. *Anat Rec* 262:380–397, 2001. © 2001 Wiley-Liss, Inc.

Key words: fossil; geometric morphometrics; *Homo erectus*; “archaic *Homo sapiens*”; Indonesia; Java

The calvaria of an “erectus-grade” hominin was recognized in early 1999 by Henry Galiano, owner of Maxilla & Mandible, Ltd., a natural history shop in New York City. As discussed by Márquez et al. (2001), the specimen ap-

parently had been recovered by dredging on the bank of the Solo River (central Java, Indonesia) near the towns of Poloyo and Sambungmacan in 1977, after which it was out of circulation until 1997. It was then placed on the antiq-

Grant sponsor: National Science Foundation; Grant numbers: BIR 9602234, ACR 9982351.

Received: 12 June 2000; Accepted: 20 December 2000

*Correspondence to: Eric Delson, Department of Vertebrate Paleontology, American Museum of Natural History, New York, NY 10024. E-mail: delson@amnh.org

uities market, briefly described (Boedihartono, 1998), and removed illegally from Indonesia. It has now been returned to that country and is catalogued as Sm 3 in the Laboratory of Paleoanthropology, Gadjah Mada University, Yogyakarta (Fig. 1).

The age of this specimen is entirely unknown at present. Galiano removed some apparently in situ matrix from the interior of the calvaria, and this has been submitted to Dr. Carl Swisher III (Berkeley Geochronology Center) for geochronometric and trace-element analysis. Two other specimens have been recovered from the Sambungmacan region, at "locality 1" (as opposed to locality 2 for Sm 3): Sm 1 is a partial calvaria (Jacob, 1975), while Sm 2 is a partial tibia (Baba et al., 1990). The exact horizons of these fossils within the Sambungmacan section are not known. Jacob et al. (1978) reported only normal geomagnetic polarity in the Sambungmacan section, suggesting either a correlation to the Jaramillo subchron (Jacob's preference, now dated to ca. 1 million years ago [Ma]) or a level within the Brunhes chron (younger than 780 ka [thousand years ago]). Matsu'ura et al. (2000) have reported trace element analyses which suggest that Sm 2 derived from the Kabuh Formation. Pending further studies, it is only possible to suggest that all three Sambungmacan fossils probably date between 1 Ma and 100 ka.

The morphology of the Sm 3 calvaria and its paleoneurology have been described respectively by Márquez et al. (2001) and Broadfield et al. (2001), and here we undertake an analysis of its phylogenetic and systematic position using both three-dimensional (3D) geometric morphometric and comparative morphological analyses.

MATERIALS AND METHODS

3D Geometric Morphometric Analysis

The first part of this study is a comparative analysis of the external midsagittal outline as well as five midsagittal landmarks of Sm 3. The comparative specimens are listed in Table 1. They include mixed-sex samples of two modern *Homo sapiens sapiens* regional populations, eleven specimens generally identified as *Homo erectus* and two individuals often termed "archaic *Homo sapiens*" (or *H. heidelbergensis*). These latter specimens, Kabwe (Zambia, estimated to date ca. 500 ± 200 ka) and Petralona (Greece, ca. 350 ± 150 ka), probably do not belong to the same phyletic lineage or to the same (sub) species. They have been united here informally in order to provide a comparative sample morphologically (and temporally) intermediate between living *H. s. sapiens* and *H. erectus*, mainly as a reflection of the limited number of western Old World Middle Pleistocene specimens available to us.

3D coordinates were recorded in a Microsoft Excel spreadsheet using a Microscribe 3DX multijoint-arm digitizer (Marcus et al., 1997). The five midsagittal landmarks recorded were glabella, bregma, lambda, inion, and opisthion. These landmarks were located (following standard definitions in Howells, 1973, and White, 2000) by direct observation, with reference to descriptive publications and minimal reconstruction of damage. Selected interlandmark distances on the casts were compared to published values to confirm the reliability of the casts. Points were also recorded at approximately 2 mm intervals between the five landmarks along the outer sagittal profile, producing four line segments. Coordinates were taken on the modern crania and on casts of the fossil specimens, including Sm 3. The modern human specimens whose sex was

not known were sexed by us using cranial features, as were the "archaic *Homo sapiens*." The *H. erectus* specimens were sexed following Weidenreich (1943, 1951) and Santa Luca (1980). Where these authors disagreed, the specimens were coded as "unknown sex."

The 3D coordinates were converted to two-dimensional (2D) coordinates by projecting the approximately sagittal points on the plane of the first two principal components of the 3D coordinates. The four line segments between the five landmarks for each specimen were joined together to form a single set of points from glabella to opisthion. The raw coordinates of those points were resampled to yield the final midsagittal profile for line analysis; this consisted of 50 "semi-landmarks" (100 coordinates) for each specimen (Bookstein et al., 1999).

Both the landmark and line coordinate data for each specimen were fitted by Procrustes superimposition (Bookstein, 1997, 1998; Bookstein and Green, 1994; Bookstein et al., 1999) using two fitting criteria: Least Squares Fit or Generalized Procrustes Analysis (GPA, formerly termed GLS) and Generalized Resistant Fit (GRF) (Rohlf, 2000; Rohlf and Slice, 1990). Both procedures scale the points for size and standardize their position and orientation. The computer program GRF-ND (Slice, 1993) was used to calculate fitted coordinates under the GRF model, and the programs tpsReg and tpsRelw (Rohlf, 1998a,b) were used in combination to calculate GPA coordinates. The coordinates obtained by these two fitting methods were analyzed separately and yielded similar results. As the shape space model is not known for GRF (Bookstein, 1996), only the GPA analysis will be discussed. The GPA results from the tps programs also provide a clear tangent space projection for statistical analysis.

In Fig. 2a, the fitted (or aligned) semi-landmarks are plotted as mean profiles for the main geographical samples, with the approximate positions of the original landmarks interpolated between the neighboring semi-landmarks. In both analyses, Sm 3 falls closest to the consensus (average) configuration of all specimens analyzed. This appears to be a stochastic result indicative of the generally "intermediate" nature of Sm 3's morphology in the sagittal midline and the number of specimens compared. It is noteworthy that the sagittal outlines of the two "archaic *H. sapiens*" specimens overlapped with those of the *H. erectus* specimens. Fig. 2b shows the ranges of variation when the semi-landmarks for all individual specimens are plotted. Several statistical tests were performed on the fitted coordinates for both the landmark and semi-landmark data, and they will be discussed in that sequence.

RESULTS

Landmarks Analysis

Centroid Size (CS) is the square root of the sum of the squared distances of each landmark from the centroid, which is effectively the center-of-mass of all landmarks for a specimen. CS is a measure of overall size of the specimen. An Analysis of Variance (ANOVA) on CS found no significant taxon, sex, or combined taxon/sex effects.

A principal components analysis (PCA) on the 10 coordinates of the 5 landmarks showed a clear separation between the fossil and the modern human groups along PC1, which explained 60% of the variance (PC2 explained 15%, PC3 12%, and PC4 0.7%). On a plot of PC2 and PC1, the two "archaic *H. sapiens*" fossils fall close together but

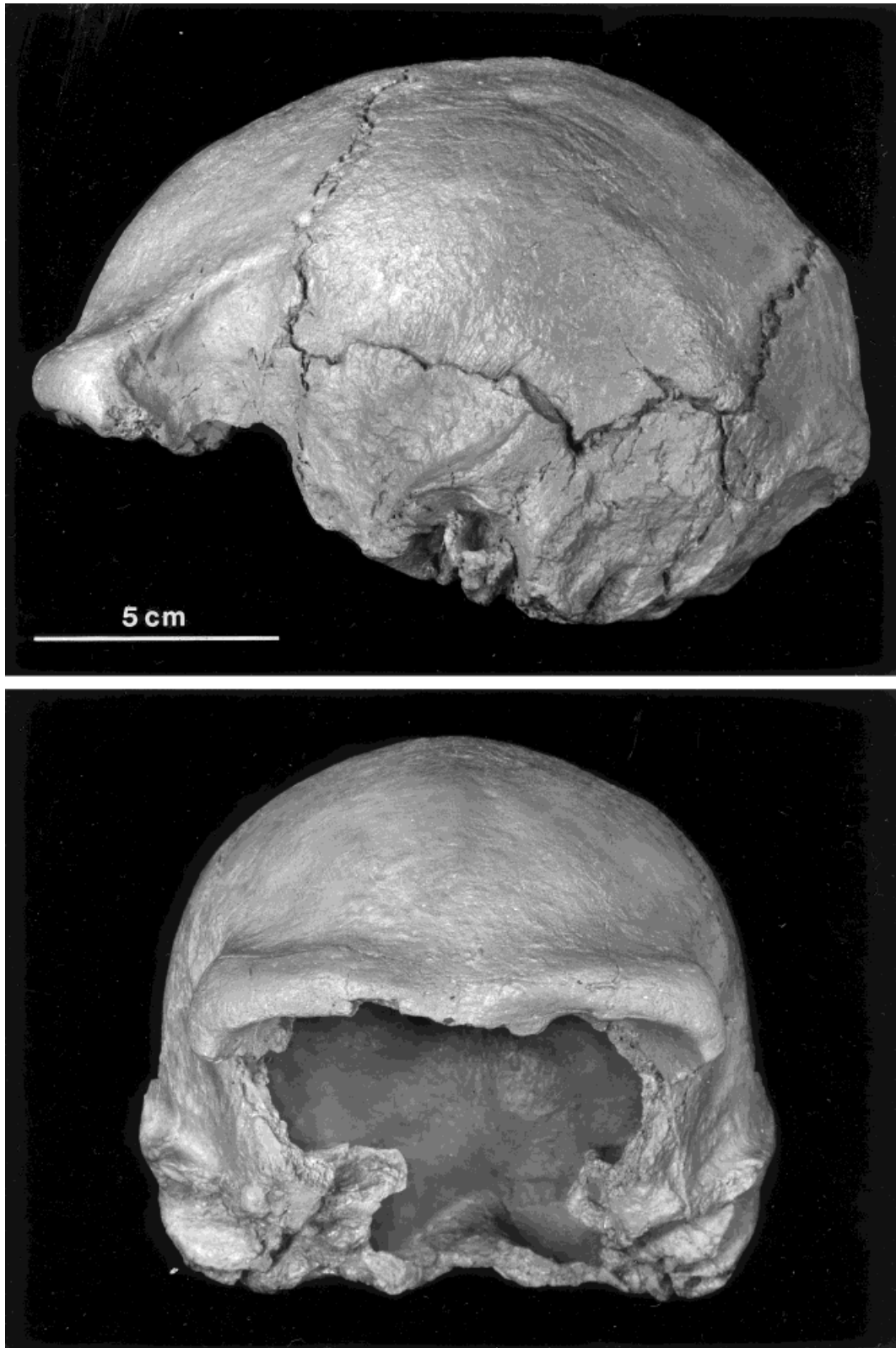


Fig. 1. Left lateral (above) and frontal views of Sm 3 (cast).

TABLE 1. Specimens included in the analyses and estimated sex

<i>H. erectus</i>		"Archaic <i>H. sapiens</i> "	
Ngandong 1	Female	Kabwe	Male
Ngandong 6	Male	Petalona	Male
Ngandong 7	Female		
Ngandong 10	Unknown sex		
Ngandong 11	Unknown sex	Modern <i>H. sapiens</i>	
Ngandong 12	Male	5 Chinese	3 M, 2 F
Sambungmacan 1	Male (??) ¹	5 Tasmanians	3 M, 2 F
Trinil 2	Female (?) [*]	(AMNH Anthropology)	
Sangiran 2	Female [*]		
Sangiran 4	Male [*]		
Sangiran 12	Unknown sex [*]		
Sangiran 17	Male		
Zhoukoudian 11	Female		
Zhoukoudian 12	Male		
ER 3733	Female		
ER 3883	Female [*]		
WT 15000	Male (juvenile) [*]		
OH 9	Male [*]		

^{*}Indicates specimen not included in geometric morphometric analysis.

¹Glabella and opisthion estimated on Sambungmacan 1.

within the range of *H. erectus*. Sm 3 is intermediate between the fossil and modern groups, but closer to the fossils. ANOVAs were conducted to test for taxon, sex, and combined taxon/sex effects on PC1 to 4. A highly significant taxon effect was detected for PC1 ($P < 0.0001$). PC2-4 showed no significant taxon effects, and none of the PCs showed significant sex or sex-taxon effects. The largest eigenvector coefficients for PC1 were those for bregma, followed by glabella and inion.

A Canonical Discriminant Analysis (CDA — SAS Institute, 1989) with four a priori groups (*H. erectus*, "archaic *H. sapiens*", modern *H. sapiens* and Sm 3), using the scores on the first four PC's as variables, separates the modern specimens from the fossils on the first canonical variate (Can1), with Sm 3 intermediate but closer to the fossils and the two "archaic *H. sapiens*" specimens still within the *H. erectus* range. Can1 explained 99.3% of the variance. DA was repeated with Sm 3 treated as an unknown. Here, Sm 3 was placed in the "archaic *H. sapiens*" group (posterior probability 0.9682), and three *H. erectus* specimens were misclassified as "archaic *H. sapiens*". The Mahalanobis distances (D) among the groups together with their P values are reported in Table 2. Note that for the six comparisons a Bonferroni correction would require a P value slightly less than 0.01 for overall 0.05 significance.

Semi-landmarks (Lines) Analysis

The semi-landmark analysis included an order of magnitude more data points (100 coordinates on 50 semi-landmarks sampling the entire profile). No significant taxon, sex, or taxon/sex effects were detected in an ANOVA on the line CS data. However, among all specimens, the smallest CS is found in ER 3733, followed by Sm 3 and a modern female Tasmanian. If small size is an indicator of sex, this finding weakly supports identification of Sm 3 as a female.

For the PCA on the semi-landmark data, the modern human specimens again were clearly separated as a group from the fossils along PC1, which explained 83% of the total variance (with 8.5% for PC2, 3% for PC3, and 2% for

PC4). The two "archaic *H. sapiens*" were not separated from *H. erectus* on any plots of these PCs. On a plot of PC2 against PC1 (Fig. 3), Sm 3 was located between the modern and fossil groups but closer to the fossils. As CS was removed during fitting, PC1 does not reflect differences in CS, but it could still reflect shape differences correlated with CS. CS was plotted against PC1, but no correlation was observed. A regression analysis was then performed on CS and PC1, which gave a r^2 value of 0.013, indicating a very low probability that variation in CS explains variation in PC1. PC1 therefore does not reflect shape differences correlated with CS. PC1 was driven by the morphology of the lower frontal, including the brow and the most inferior 1–2 cm of the frontal squama, the cranial vault at the parietals, the iniac region on the occipital and the lower occipital scale (see also Fig. 1). Using tpsRelw, it was possible to determine the idealized "endpoints" of the shape variation expressed by PC1, indicating that a low score (as for the fossils) represented a low and elongate neurocranium, while a high score on PC1 (as for the modern humans) reflected a higher, more rounded vault. PC2 to 4 were also examined, but no group separation was observed. ANOVAs conducted to test for taxon, sex, and

TABLE 2. Mahalanobis D distances among hominin groups studied, derived from canonical discriminant analysis of scores on first four principal components—landmarks and lines

	Sm 3	<i>H. er.</i>	arch. <i>H. s.</i>	mod. <i>H. s.</i>
Sm 3	0	4.208*	3.297	6.634***
<i>H. er.</i>	3.370	0	1.450	10.373***
arch. <i>H. s.</i>	3.642	1.897	0	9.614***
mod. <i>H. s.</i>	5.332**	8.684***	8.527***	0

Significance: * $P < 0.05$; ** $P < 0.01$; *** $P < 0.001$ (not Bonferroni corrected).

Abbreviations: *H. er.*, *Homo erectus*; arch. *H. s.*, "Archaic *H. sapiens*"; mod. *H. s.*, modern *H. sapiens*.

Landmarks analysis results above the diagonal, semi-landmark results below.

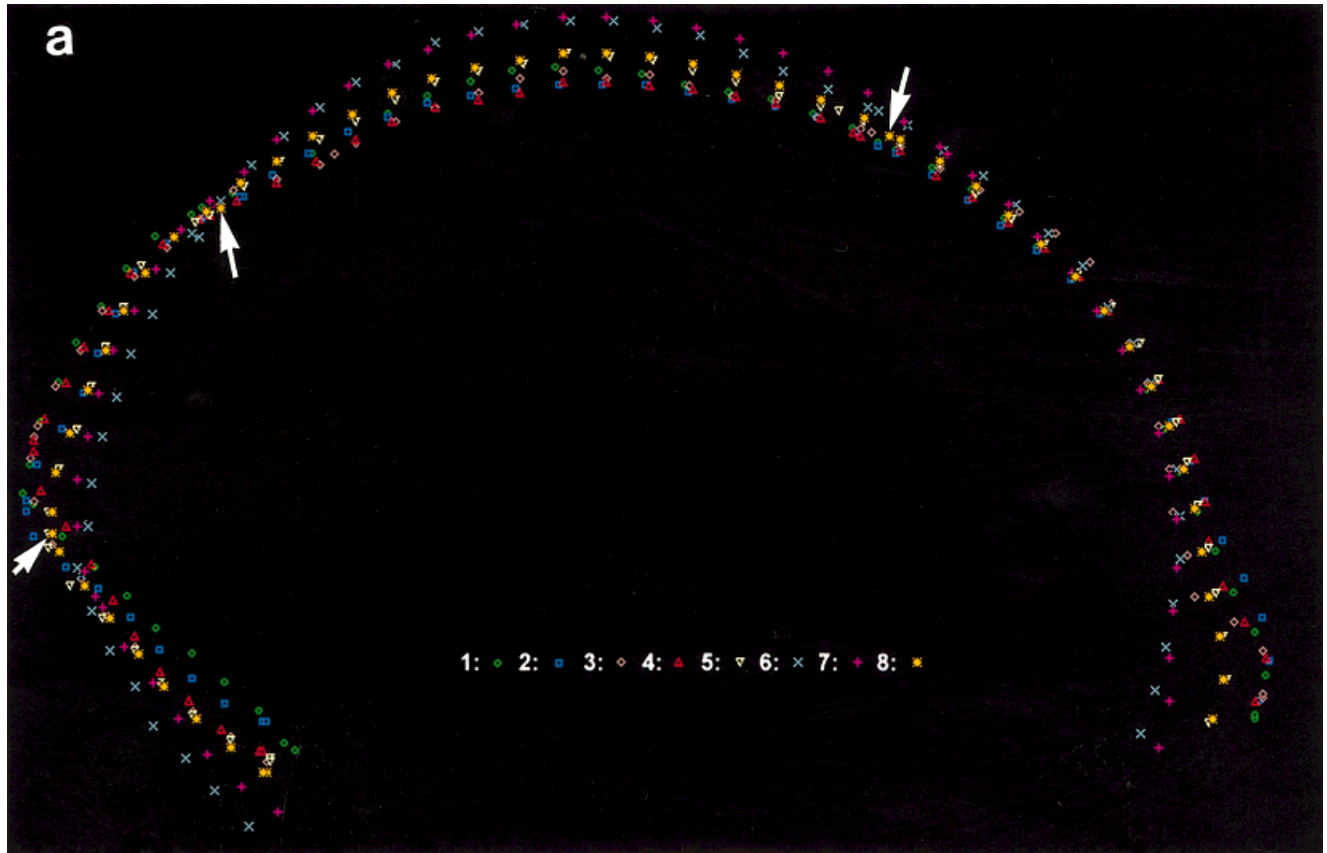


Fig. 2. (a) Sagittal profile outlines of group means and overall average (consensus) of semi-landmarks fitted by Generalized Procrustes Analysis, with positions of landmarks interpolated. Note the placement of Sm 3 intermediate between the fossil and modern samples, nearly coincident with the consensus, as well as the lack of distinction between the two fossil samples. 1: "archaic *H. sapiens*;" 2: Indonesian *Homo*

erectus (Sangiran 17, Sambungmacan 1, Ngandong 1, 6, 7, 10, 11, 12); 3: African *Homo erectus* (ER 3733); 4: Chinese *Homo erectus* (ZKD 11, 12); 5: Sm 3; 6: modern North Chinese; 7: modern Tasmanians; 8: consensus (grand mean). (b) Sagittal profile outlines of semi-landmarks for individual specimens fitted by Generalized Procrustes Analysis.

combined taxon/sex effects on PC1 to 4 revealed for PC1 a highly significant taxon effect ($P = 0.0001$), as well as a marginally significant sex effect ($P = 0.047$). A significant sex effect was also detected for PC4 ($P = 0.0087$). No other significant effects were observed. In a plot of PC1 vs. PC4, there is a slight tendency for females to score lower on PC1 and higher on PC4 within their groups. Thus, the few fossils identified as female tend to more closely approach the modern group. Sm 3 lies in a somewhat isolated position, but if it is considered *Homo erectus* (see below) then this analysis again marginally supports its identification as female. However, since sexing of the fossil specimens is highly problematic, this result is tentative at best.

A CDA was performed with the specimens placed into the same four groups as above. Can1 (which explained 98.6% of the variance) again separated the modern specimens from the fossils, with Sm 3 again intermediate but closer to the fossils. The two "archaic *H. sapiens*" specimens were within the *H. erectus* scatter (Fig. 4). Can2 explained only 1.4% of the variance, but all Ngandong specimens had negative scores, while all other fossils (including Sm 1 and Sangiran 17) scored positively (with Petralona having the highest score of any specimen); Sm 3 fell within the Ngandong range on Can2. Interestingly,

the modern human crania were also separated by population, the Tasmanians scoring above 0.13 and the Chinese below 0.20. When Sm 3 was treated as an unknown, it was classified as *H. erectus* with a posterior probability of 0.722. Two *H. erectus* specimens were misidentified as "archaic *H. sapiens*", but all other specimens were correctly identified. The Mahalanobis D distances among the groups are reported in Table 2.

Additional statistical tests were undertaken on the Procrustes distances (the square root of the sum of the squared distances between corresponding positions of semi-landmarks when the specimens have been optimally superimposed). Fig. 5 displays a plot of the Procrustes distances among the means of the four groups, with a minimum spanning tree superimposed (Rolf and Marcus, 1993). This reveals the relative isolation of modern humans and the intermediate position of Sm 3 between "archaic *H. sapiens*" and *Homo erectus*.

A permutation test on the Procrustes distances (see Bookstein et al. 2000) was conducted to examine the probability that inter-group differences as large as those observed for the known groups could be obtained through random permutations of specimen membership in the named groups (see Table 3). For 1,000 permutations, the

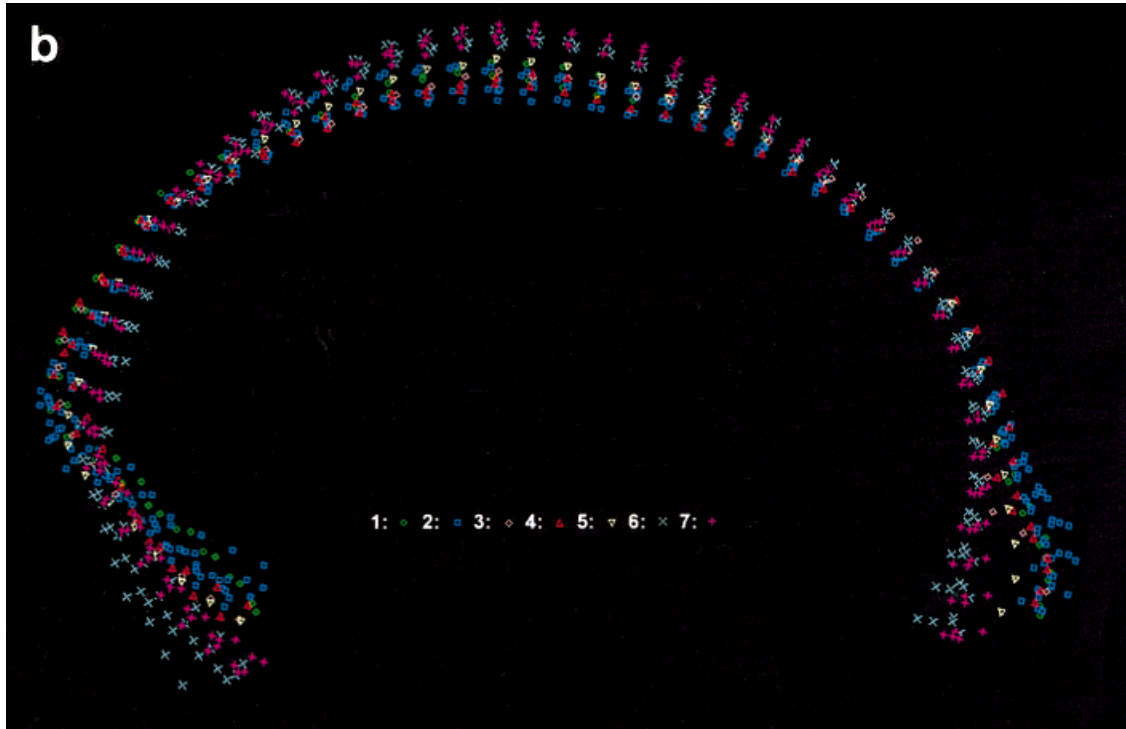


Figure 2b.

test showed that the Sm 3 to *H. erectus* distance was marginally significant ($P = 0.043$). Thus, there was a less than 5% chance that the difference between Sm 3 and the *H. erectus* mean could be randomly exceeded, i.e., it was unlikely that Sm 3 should be included in *H. erectus*. All the distances to *H. s. sapiens* are never exceeded by the random permutations, thus it is highly unlikely that any of the fossil groups could be included within *H. s. sapiens*. On the other hand, the distances from “archaic *H. sapiens*” to both Sm 3 and *H. erectus* were nonsignificant; thus, either of the latter two could possibly be included within “archaic *H. sapiens*”. If a Bonferroni correction (modified or complete; see Rice, 1989) was applied to these values, the distance between Sm 3 and *H. erectus* would no longer be significant, and therefore the two samples could potentially have been drawn from the same larger population. The permutation test can be characterized as more conservative than those discussed above (because it requires fewer assumptions about the underlying data), but in this case its result is less definitive. A permutation test was also conducted on the landmark Procrustes distances (Table 3, above diagonal). The results were similar, although most of the probabilities were higher; given the lower information content of the landmark data, these results are not considered further.

LANDMARK AND SEMI-LANDMARK ANALYSIS DISCUSSION

The analyses of landmarks and semi-landmarks yielded similar results except for the DA identification of Sm 3. The landmark analysis identified Sm 3 as “archaic *H. sapiens*”, while the line analysis identified it as *H. erectus*. Both analyses failed to clearly distinguish between *H.*

erectus and “archaic *H. sapiens*”, and both misidentified some *H. erectus* specimens as “archaic *H. sapiens*”. The source of this error can be seen in the plot of the outlines (Fig. 1), where “archaic *H. sapiens*” overlaps with *H. erectus* along the entire midsagittal outline. However, the line analysis based on PCA scores achieved a better resolution, with larger D between the two fossil groups and with fewer specimens misidentified. The Procrustes distance analysis of line data also indicated a closer similarity of Sm 3 and *Homo erectus*, although the permutation test results were less clear. A shortcoming of the landmark analysis was the small number of points used. The addition of landmarks (or lines) away from the midsagittal plane would also probably enhance the analysis, yielding greater separation of the groups, especially among the fossils. Such an extension of this work is planned, but will be difficult because some landmarks such as porion and asterion are not easily located on many of the available casts (although they might be on the original fossils).

Modern humans are clearly different in the shape of their midsagittal outline from all the fossil human specimens measured (Fig. 2a). Glabella is depressed and the brow region is flat even in the Tasmanian specimens with a comparatively heavy browridge. The lower frontal squama (=supratatorial plane) is also depressed compared to the fossils. Interestingly, the modern and fossil human ranges converge superiorly and completely overlap in the upper part of the frontal and up to bregma (located between semi-landmarks 17 and 18). (These patterns and those that follow are true of both the GPA and the GRF analyses.) The profiles of the modern and fossil (other than Sm 3) groups diverge posteriorly on the parietals, where the former show a much higher and more rounded outline than the latter. The modern and

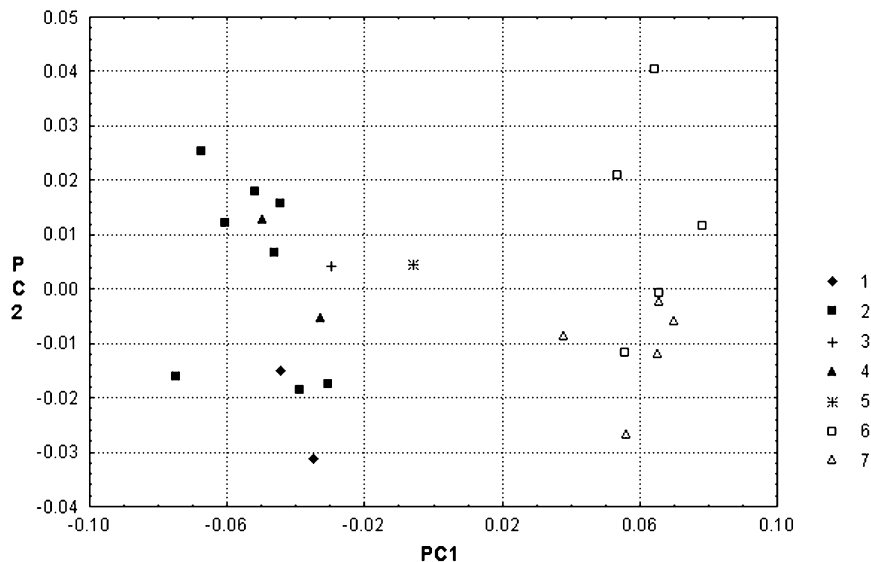


Fig. 3. Plot of results of the principal component analysis (PCA) of line (semi-landmark) Procrustes fitted coordinates. PC1, on the x-axis, explains 83% of the variance, while PC2 explains 8.5%. Group numbers as in Fig. 2.

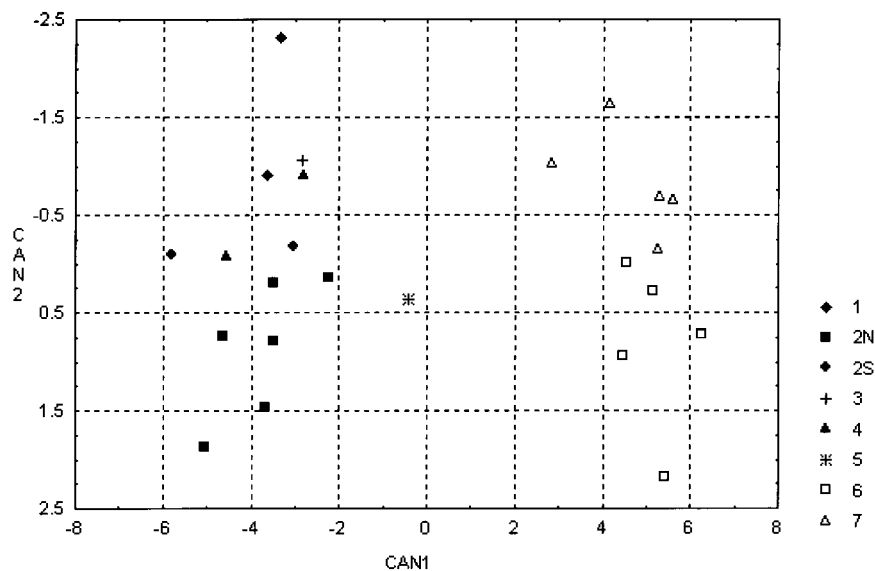


Fig. 4. Plot of results of canonical discriminant analysis (CDA) of scores on PC1–4 (see text and Fig. 3) from semi-landmark analysis. Can1, on the x-axis, explained 98.6% of the variance, while Can2 explained about 1.4%. Group numbers as in Fig. 2.

fossil outlines cross again near lambda (between semi-landmarks 33 and 34), with the modern humans showing a flatter occiput and a less posteriorly protruding inion. These outlines cross a third time near or just below inion, with the fossils showing a greater angulation between the upper and lower occipital scales. Inion is an observationally determined point (rather than one defined by bony contacts), and it falls much lower in modern humans than in the fossils.

The close approximation of the semi-landmark lines at lambda, and to a lesser degree at bregma, suggests that evolutionary change in the shape of the vault is possibly

constrained by the growing margins of the parietal, rather than being equally likely at any point along the midsagittal arc. Further examination of this potentially important pattern is planned through analysis of landmarks and semi-landmarks around the margins of the frontal, occipital, parietals, and temporals.

One of the most striking paleoanthropological results of this study is the intermediate character of the midsagittal outline of Sm 3 as noted above. In Fig. 2a, Sm 3 is nearly coincident with the grand mean of all specimens and is seen to be intermediate in all of the cranial

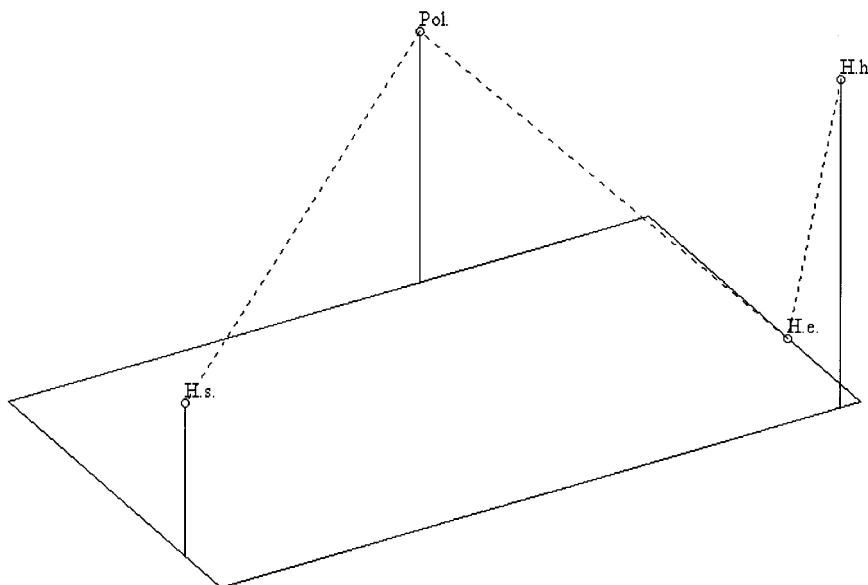


Fig. 5. Plot of the Procrustes distances among the means of the four studied groups, with a minimum spanning tree superimposed. **H. h.**, "archaic *H. sapiens*"; **Pol**, Sm 3; **H. e.**, *Homo erectus*; **H. s.**, modern humans.

TABLE 3. Permutation test probabilities for Procrustes distances between means

	Sm 3	H. er.	arch. H. s.	mod. H. s.
Sm 3	1	0.398	0.660	0.020
H. er.	0.043	1	0.408	0.000
arch. H. s.	0.189	0.177	1	0.000
mod. H. s.	0.000	0.000	0.000	1

Group Abbreviations: H. er—*Homo erectus*; arch H. s.—"Archaic *H. sapiens*"; mod. H. s.—modern *H. sapiens*. Landmarks above diagonal, lines below diagonal.

regions separating modern humans from the fossil specimens. Its glabella is depressed relative to those of the other fossils, but protrudes more anteriorly than the modern specimens. There is no postorbital sulcus or flattening. The curvature of the vault at the parietals is higher than in the fossil group means, but is still clearly separated from the modern human population means. Its inion is less posteriorly protruding than the fossil group mean outlines, and shows a weaker angulation between the upper and lower occipital scales than the fossil mean outlines but more than the modern means. However, when all of the individual specimens are plotted (Fig. 2b), it can be seen that the Sm 3 midsagittal outline falls at the extreme of the fossil specimens' range of variation in all of these regions except the brow. Sm 3's depressed glabella and brow ridge, as well as the steepness of its supratoral plane, are unique among the fossil specimens included in this analysis, and are truly intermediate between the fossil and modern groups examined. The small size of the Sm 3 specimen, the gracile morphology of its brow region in the midsagittal profile, and its position on the PC plots combine to suggest that it may have been a female

individual. The lack of separation between *Homo erectus* and "archaic *H. sapiens*" makes it difficult to assign Sm 3 to one of these two samples rather than the other. The permutation test in the line analysis weakly suggests a greater likelihood of the latter, while the discriminant analysis more reliably points to the former. In sum, the overall indication is that, in terms of its sagittal profile, Sm 3 probably represents a morphologically distinctive small female *Homo erectus* individual, though this is not strongly supported.

COMPARATIVE MORPHOLOGY OF SM 3 AND OTHER FOSSIL HOMININS

The overall morphology of Sm 3 is similar to that of other *Homo erectus* specimens, sharing over 50% of the more common morphological traits associated with the African, Asian, and Indonesian *H. erectus* groups. Table 4 lists some of the more commonly cited apomorphies of *H. erectus* and indicates which of them are known for Sm 3. Among Asian *H. erectus* specimens, Sm 3 is most similar to the specimens thought to be female, with greatest similarity to the Javanese material, especially the specimens from Ngandong and Sambungmacan. Table 5 provides a selection of linear measurements from several sources for comparison with Sm 3. The second half of this paper is a preliminary assessment of some aspects of the morphology of this fossil based on direct comparisons of casts (see Table 1). The morphometric results above served as a guide for this analysis, while a complete description is provided by Márquez et al. (2001).

Comparative Description

Supraorbital region. The supraorbital torus of Sm 3 is rather gracile, especially in its medial portions. The glabellar torus does not project as far anteriorly as do the superciliary arches, but is relatively depressed, forming a

TABLE 4. Some craniofacial characters typical of *Homo erectus (sensu lato)*¹

- A thick and continuous supraorbital torus with a supratotal sulcus
- **Frontal and anterior parietal keeling along the midline**
- The presence of an angular torus on or near the mastoid notch
- **The occipital squama is wide** and sharply angled
- A linear transverse occipital torus
- **A narrow mandibular fossa that produces a deep fissure between the entoglenoid pyramid and the tympanic plate**
- The tympanic bone terminates medially in an infratubarius process
- **A fissure separates the petrosal crest from the mastoid**
- **Vault bones are relatively thickened**
- **Endinion and inion are widely separated**
- **Endocranial volume approximately 1000 cc**
- Occipital plane is shorter in sagittal length when compared to the nuchal plane
- **The presence of an occipitomastoid ridge**
- **A foramen magnum that is posteriorly positioned**
- Absence of a paramastoid ridge
- **Well developed suprasmatal crest (tegmen)**
- **Absence of a vaginal crest**
- **Absence of a postglenoid process**
- **Absence of a styloid process**
- Absence of foramen lacerum
- **Low temporal squama**
- **Lateral wing on the supraorbital torus**

Bold indicates characters exhibited by Sm 3.
¹Sources: Weidenreich (1943, 1951); Jacob (1975, 1976); Macintosh and Larnach (1972); Santa Luca (1980); Andrews (1984); Stringer (1984); Wood (1984, 1991); Rightmire (1990); Dean (1993).

midline glabellar concavity (Santa Luca, 1980). In this respect Sm 3 is similar to Ngandong 7, 11, 12 and Zhoukoudian 12 (although this last specimen shows a very slight concavity). It is different from Ngandong 1, 6, 10, Sangiran 17, Zhoukoudian 11, and the "archaic" specimens Kabwe and Petralona, where the glabellar torus projects markedly anteriorly and is continuous with the medial portions of the superciliary arches. Slight glabellar concavities are also present in the African *H. erectus* fossils OH 9, ER 3733, and ER 3883 (although the latter specimen shows deformation in the left supraorbital torus). The superciliary arches of Sm 3 do not project as far anteriorly as those of the other specimens, making its glabellar concavity appear rather shallow and wide in superior view. Unfortunately, it is impossible to assess the slope of the glabella to nasion profile in Sm 3, as the bone is broken just inferior to glabella.

The supraorbital torus of Sm 3 becomes thicker superoinferiorly at the lateral end of the supraorbital trigone, so that the thickest part of the torus is near the zygomatic process of the frontal. This morphology is similar to that of the Ngandong fossils. It differs from that in Zhoukoudian 2, 3, 10, 11, and 12, Sangiran 17, ER 3733 and 3883, OH 9, Kabwe, and Petralona, where the torus is either uniform in thickness or is thickest more medially (Weidenreich, 1943; Santa Luca, 1980; Wood, 1991). Rightmire (1993) provided measurements which suggest a different interpretation, but he did not discuss this matter in his

TABLE 5. Measurements (in mm) of selected cranial variables in Sm 3 and other *Homo erectus*

	Sm 3	Sm 1	Ng 1	Ng 6	Ng 7	Ng 11	Ng 12	Sgr 2	Sgr 4	Sgr 10	Sgr 12	Sgr 17	Trinil 2	Java Range	ZKD Mean	ER 3733	OH 9
Gl-Ops (C)	179	200	197	219	191	203	201	177	—	—	—	206	183	177-219	194	182	205
Ft-Ft (C)	101	102	—	102	101	110	101	79	—	83	94	99	85	79-102	86	91	(100)
Max BiPar (C)	127	146	—	147	142	149	142	134	136	130	139	144	—	127-149	134	127	138
Po-Po (C)	132	—	—	—	—	—	—	114	120	—	126	130	—	114-132	124	121	125
Au-Au (C)	134	137	—	151	141	151	144	131	136	129	142	150	126	129-151	136	135??	—
Gl-Br (C)	103	115	112	116	103	111	104	—	—	—	—	108	—	103-108	107	95	(120)
Gl-Br (A)	106	—	117	120	107	117	107	—	—	—	—	113	—	106-120	113	106	(128)
Br-La (C)	98	96	106	109	96	102	92	90	89	93	82	106	88	82-109	95	(83)	—
Br-La (A)	105	102	114	115	109	111	104	94	90	100	86	109	91	86-115	101	(83)	—
La-In (C)	50.5	59	52	59	59	57	66	45	51	49	48	58	—	45-66	49	61	—
La-In (A)	54	—	53	61	62	60	69	47	57	52	55	63	—	47-69	—	68	—
In-Op (C)	40.1	—	52	63	51	57	51.5	48	55	54	54	53	—	40-63	59	50	—
In-Op (A)	44	—	55	66	54	60	54	52	62	—	54	55	—	44-66	—	50	—
La-Op (C)	80.5	—	80	93	85	83	90	75	80	—	83	80	78	78-93	85	88	—
La-Op (A)	96	—	108	127	116	120	123	100	112	—	109	120	103	96-127	114	117	—
Ast-Ast (C)	118	127	127	126	123	127	126	120	135	126	125	142	92	92-142	115	124	123
Ast-Ast (A)	126	—	—	—	—	—	—	155	187	140	160	198	—	126-198	151	158	148

Abbreviations used: Sm, Sambungmachan; Ng, Ngandong; Sgr, Sangiran; ZKD, Zhoukoudian; Java Range includes only Indonesian specimens included in this table. Data for specimens other than Sm 3 taken from: Weidenreich, 1943, 1951; Jacob, 1975; Santa Luca, 1980; Rightmire, 1993; and Wood, 1991. (C), chord measurement; (A), arc measurement. Gl, glabella; Ops, opisthocranion; Ft, frontotemporale; Max BiPar, maximum biparietal breadth; Po, porion; Au, auricular; Br, bregma; La, lambda; In, inion; Op, opisthion; Ast, asterion.

text, and it is not certain that his measurements are homologous with those of the other authors.

Sm 3 shows a more gracile torus than most of the specimens examined, a feature that is consistent with female sex. The superciliary portions of the torus are thinner supero-inferiorly than those of the most gracile Asian *H. erectus* specimens, Ngandong 7 and Zhoukoudian 11, both thought to be female, but slightly thicker than in ER 3733, the African specimen also commonly referred to as female. In the trigone portion of the torus, Sm 3 is probably comparable to the damaged Ngandong 7 and similar to or slightly thicker than Zhoukoudian 11, but thicker than ER 3733.

The supratatorial region in Sm 3 is similar to that present in the Ngandong individuals in that there is no supratatorial sulcus; the supratatorial plane is straight above glabella but more concave above the trigones, where it forms relatively wide, triangular plateaus (Santa Luca, 1980). Sangiran 17 and Sm 1 show a comparable morphology in this region, although only the right trigone is preserved in the latter. The Zhoukoudian specimens differ in that they show a supratatorial sulcus, which is deepest and widest laterally but also forms a concavity above glabella. A similar and possibly even more accentuated sulcus is found in OH 9 and especially in ER 3733. ER 3883 is damaged in this region, but it appears to be more similar to the Indonesian specimens, showing a straight supratatorial plane and almost no supratatorial sulcus (Santa Luca, 1980; Weidenreich, 1943; Wood, 1991). The “archaic” specimens Kabwe and Petralona show a flat supratatorial plane, with only slight concavities above the glabellar portion.

Although Sm 3 is most similar to the Indonesian specimens in its supratatorial morphology, it differs from them in the degree of overall anterior projection of glabella and consequently also in the steepness of the supratatorial plane, which is much more vertical than any other fossil examined here (see Fig. 2). None of the other fossils approaches this condition, as is also evident from the morphometric results, where Sm 3 was shown to be truly intermediate between modern humans and fossil specimens in the region of the glabella and the lower frontal.

Upper frontal and parietal. The frontal squama of Sm 3 is much more rounded than in the Ngandong specimens, Sm 1, Sangiran 17, ER 3883, OH 9, WT 15000, Kabwe, and Petralona. It is more similar in this feature to Zhoukoudian 11, 12, and ER 3733, although the latter specimens show strong sagittal keeling which contributes to the midline curvature of the frontal. The rounded frontal outline of Sm 3 is also reminiscent of that shown by the calvaria from Ceprano, Italy, recently described by Ascenzi et al. (1996, see their Fig. 5a). Postorbital constriction in Sm 3 is not as strong as in the Zhoukoudian or African specimens, but is comparable to those from Ngandong, Ngawi, and Sm 1 (see Fig. 6).

Sm 3 presents a weakly developed frontal sagittal keel with only slight flattening of the squama on either side, which does not contribute to the rounded shape of the frontal squama. There is no bregmatic eminence or coronal ridging. Sagittal keeling is also found on the anterior part of the parietal, where it is relatively strong. The Ngandong fossils show variable expression of all these traits. Zhoukoudian 11 and 12 show stronger frontal and

parietal keeling than Sm 3, as well as a bregmatic eminence and slight coronal ridging. Sangiran 2 and 17 show strong bregmatic eminences but no frontal and only slight parietal keeling. In its preserved posterior parietal region, Sangiran 4 presents a very strong keel. Among the Asian specimens Sm 3 is most similar to Sm 1, showing a relatively weak frontal and parietal keel and no bregmatic eminence or coronal ridging. ER 3733 shows a strong frontal but no parietal keel and no coronal ridging; the area around bregma is damaged. ER 3883 presents very slight frontal and parietal keeling, but no bregmatic eminence or coronal ridges. OH 9 does not exhibit frontal keeling, and it does not preserve the parietals. Of the two “archaic *H. sapiens*” specimens studied, Kabwe shows a frontal keel and a bregmatic eminence, but no parietal keel or coronal ridges, while Petralona shows none of these features.

The gracility of Sm 3 in its sagittal and coronal ridging would seem to support its assignment to female sex. However, the proposed *H. erectus* females present a different pattern. Ngandong 7 shows the heaviest ridging of the Ngandong specimens, with strong frontal and parietal keels, a prominent bregmatic eminence and distinct coronal ridges. Zhoukoudian 11 and ER 3733 both show frontal keels that are heavier than those in Sm 3, while the former also presents a stronger parietal keel and a bregmatic eminence. The expression of the frontal keel in Sm 3 is comparable to that in Sm 1, thought to be a male, although the parietal keel in Sm 3 is stronger.

The angular torus is a traditional hallmark characteristic of *H. erectus* (Rightmire, 1993; Santa Luca, 1980; Weidenreich, 1943), and one thought by Andrews (1984) and Stringer (1984) to differentiate between African and Asian *H. erectus* specimens. No true angular torus is present in Sm 3; only a slight swelling appears at the posterior end of the superior temporal line on the posterolateral corner of the parietal, between the parietal incisure and asterion. An angular torus is well developed in Sm 1, ZKD 11, Ngandong 1, 6, 10, 11 and 12, and OH 9. It is small or entirely lacking in Sangiran 2 and 4, Ngandong 7, ZKD 12, and ER 3733 and 3883. There is disagreement over the presence of an angular torus in the “archaic” specimens studied. A distinct elevation can be seen in Kabwe at the end of the superior temporal line and between parietal incisure and the lambdoid suture. This was interpreted as an angular torus by Rightmire (1993), but not by Santa Luca (1980), who regarded it as simply a lateral extension of the occipital torus. Only a slight elevation can be distinguished in this region on the cast of Petralona. Stringer et al. (1979) and Rightmire (1993) interpreted this as a moderate angular torus, but even this view was questioned by Stringer (1984). The very slight development of this feature in Sm 3 supports its sexing as a female, as the strong expression of tori has been used to determine sex in *H. erectus* specimens (Santa Luca, 1980). On the other hand, the angular torus is more strongly developed in ZKD 11, thought to be female, than in the male ZKD 12.

Temporal. Andrews (1984; see also Stringer, 1984) considered the furrow that separates the mastoid process from the tympanic a feature differentiating Asian from African *Homo erectus*. This trait, termed “mastoid fissure” by Andrews (1984), will be referred to here as the “tympanomastoid fissure.” Sm 3 shows a well-marked tympan-

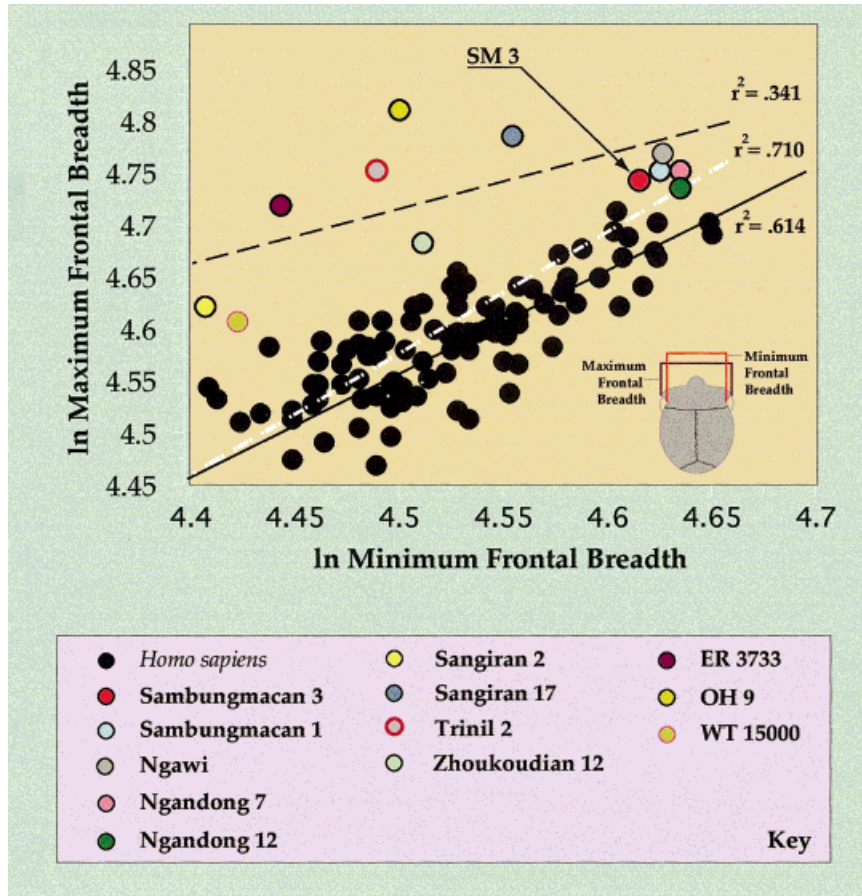


Fig. 6. Bivariate natural log plot of maximum vs. minimum frontal breadth (see Table 5) in *Homo sapiens* ($n=105$, neonate through adult) and selected *H. erectus*. Sm 3 clusters tightly with Sm 1, Ngandong 7 and 12, and Ngawi. Other *H. erectus* have stronger constrictions. Three regression lines (least squares) are shown: the solid black line is based on the modern human sample; the white dashed line adds the cluster of

H. erectus near Sm 3—note that this increases the r^2 correlation coefficient; the black dashed line is based only on the 12 *H. erectus* specimens—its low r^2 suggests great variability in this diverse sample by comparison to the modern humans. (Measurements of fossils on casts, except Sm 3 on original and Ngawi from tracing in Sartono 1990; Sangiran 2 based on doubling measures on right side.)

nomastoid fissure most similar to the morphology in the Ngandong group (e.g., 6, 7, 11, 12), where the fissure is wide with walls roughly parallel to each other (Fig. 7). This fissure is more weakly expressed in Sangiran 4 and Sm 1 and in Zhoukoudian specimens, where it is often wedge-shaped (Weidenreich, 1943). Sangiran 17 is damaged in this area. The African fossils ER 3733, ER 3883, and OH 9 do not show this feature, although the more recently recovered specimen WT 15000 shows a wide tympanomastoid fissure with parallel walls. This finding indicates that perhaps the distinction between African and Asian *H. erectus* is not as clear-cut as suggested by Andrews (1984). However, the WT 15000 specimen is subadult, and it is possible that the morphology of this region would change with growth completion. Among the “archaic *H. sapiens*” specimens examined, Kabwe shows no tympanomastoid fissure, while Petralona does not preserve this region.

Sm 3 also shares with the Ngandong specimens the distinct morphology and relative position of the squamotympanic fissure (Fig. 7). In his description of the Ngandong crania, Weidenreich (1951, p. 273–274) noted both

the deep and antero-posteriorly short shape of the mandibular fossa and the course of the squamotympanic fissure (which he mistakenly termed the “Glaserian” fissure; see Márquez and Mowbray, in preparation) as being characteristic for this group. He observed that in the Ngandong specimens and in Sangiran 4 the squamotympanic fissure courses mediolaterally and coincides with the deepest portion of the mandibular fossa, whereas in the Chinese *H. erectus* specimens and in modern humans this fissure is positioned more posteriorly, and the floor of the fossa descends toward the posterior wall before reaching the fissure. In the last 50 years, many additional *H. erectus* crania preserving this region have been recovered. The Indonesian specimens Sangiran 17 and Sm 1 show a morphology similar to that preserved in the Ngandong group. The African representatives are divided in the expression of this feature. ER 3733 and 3883 have a flat and antero-posteriorly long mandibular fossa and a squamotympanic fissure that runs posterior to the deepest portion of the fossa. WT 15000 also shows a flat and long fossa, but the squamotympanic fissure courses in its deepest portion. However, it is noted again that growth has not been com-

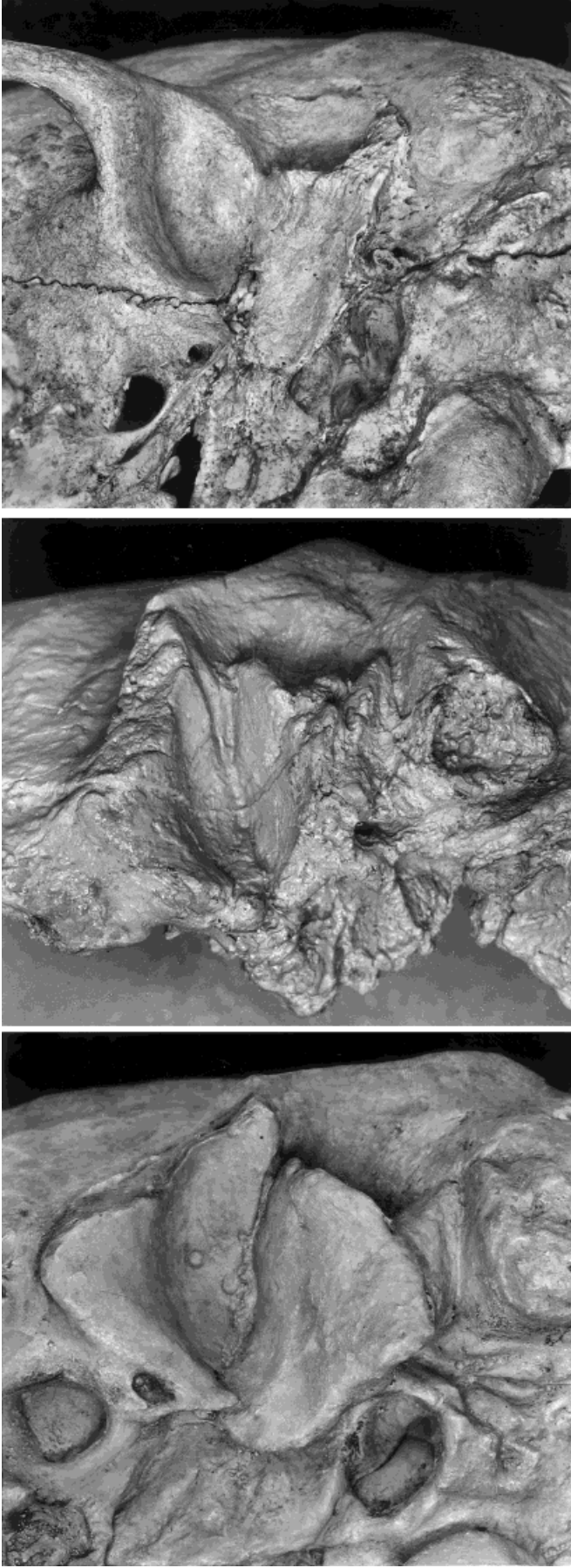


Fig. 7. Basal view of the right mandibular fossa in (left to right) Ngandong 7 (cast), Sm 3 cast, modern Tasmanian. Note the mediolateral course of the squamotympanic fissure in the deepest portion of the fossa and the wide typanomastoid fissure with roughly parallel walls in Ngandong 7 and Sm 3.

pleted in this specimen (see above). Finally, OH 9 presents a mandibular fossa that is similar both in its shape and in the position of the squamotympanic fissure to the Ngandong and other Indonesian specimens. It appears that this trait unites the Indonesian *H. erectus* specimens to the exclusion of the other Asian and African ones, with the exception of OH 9 and possibly also WT 15000. Kabwe shows a squamotympanic fissure that courses posteriorly to the deepest portion of the mandibular fossa, while this region in Petralona is still partially covered with matrix, making evaluation of this trait difficult. This aspect of the mandibular fossa morphology of Sm 3 aligns it with the other Indonesian specimens.

The suprameatal and supramastoid crests of Sm 3 are prominent on both sides and mark the point of greatest cranial breadth. Posteriorly, the supramastoid crest courses upward at an angle to the suprameatal crest and crosses the squamosal suture above the parietal incisure. It is separated completely from the mastoid crest by a wide and shallow supramastoid sulcus. This condition is similar to that seen in the Ngandong fossils. It differs from the morphology shown by the Zhoukoudian specimens, where the supramastoid crest continues along the axis of the suprameatal crest and crosses the squamosal suture at or just above the parietal incisure, and where there is no supramastoid sulcus (or only a very slight one) separating the mastoid and supramastoid crests (Santa Luca, 1980; Stringer, 1984). Sangiran 2 and 17 follow the Zhoukoudian pattern, while Sangiran 4 (following Santa Luca, 1980) and Sm 1 are similar to Ngandong. The African specimens all exhibit morphology similar to that seen in Zhoukoudian, and a slight supramastoid sulcus is found only in ER 3733. Kabwe and Petralona show a straight supramastoid crest, but the former also presents a narrow supramastoid sulcus. The presence of such a sulcus in Petralona cannot be assessed due to damage in this region.

The development of the suprameatal and supramastoid crests in Sm 3 is comparable to that seen in ZKD 11 and especially 12, Sangiran 17 (and perhaps the damaged Sgr 4), and Sm 1. In the Ngandong sample the suprameatal crest is strong, but the supramastoid crest is variably developed: Ngandong 7 presents a diffuse supramastoid swelling instead of a supramastoid crest; in Ngandong 12, the crest is strong but flattened or blunt; and in Ngandong 6 and 10 it is comparable to that shown by the Sangiran specimens. The African *H. erectus* fossils, including OH 9 despite its great overall robusticity, present weak supramastoid crests. Among the "archaic" specimens, Kabwe is similar to the African specimens, while Petralona shows a swelling comparable to but more prominent than that of Ngandong 12. It is not clear how this trait is related to sex; the prominent supramastoid crest in Sm 3 could be an indication of male sex.

Occipital. Although Sm 3 possesses a relatively robust occipital torus (which may be slightly eroded), it shows a less sharply angled occiput than most of the other fossils, including the "archaic *H. sapiens*" Kabwe and Petralona (see also morphometric results). The occipital torus is relatively thick supero-inferiorly, and it is most similar in this dimension to Ngandong 7. The superior margin of the central part of the Sm 3 occipital torus is not straight in posterior view, as in the Zhoukoudian sample, Sangiran 2 and 17, ER 3733, and OH 9, but it is arched, as in the

Ngandong and Sm 1 specimens. It is separated from the occipital squama by a slight furrow that dips inferiorly in the midline. This furrow is different from the well-marked horizontal supratoral sulcus present in the Zhoukoudian fossils. It also differs from the morphology present in Ngandong and Sm 1, where the transition from the occipital plane to the occipital torus is marked by a smooth concavity, which in Ngandong 1, 6, 10, and 11 results in a shelf-like appearance of the superior toral margin. No clear furrow or concavity can be seen in the African fossils or in Sangiran 2 and 17. Although the surface of the bone is slightly eroded in Sm 3, the occipital torus appears to project away from the squama only slightly, much less so than in the Ngandong series, where this trend is most pronounced, but also less than in Sm 1, ZKD 11, and ZKD 12. It does project further, however, than in Sangiran 2 and 17 and ER 3733.

Inferiorly, Sm 3 shows excavation of the nuchal scale marking the attachment of the nuchal musculature; an external occipital crest is present. A strong excavation of the nuchal scale and the presence of an external occipital crest are characteristic of the Ngandong fossils, and appear even in the relatively gracile putative female Ngandong 7 (Santa Luca, 1980; Rightmire, 1993). Relatively strong muscular impressions are also seen in Sm 1, but these are shallower than those present in the more robust Ngandong crania; the external occipital crest area is damaged. The Zhoukoudian sample and Sangiran 2 show very faint impressions of the nuchal musculature and no or very little development of the external occipital crest. The muscular impressions are also faint in Sangiran 17, ER 3733, WT 15000, and OH 9, although a small external occipital crest is present. The nuchal excavation in Sm 3 is less pronounced than in any Ngandong specimen or Sm 1, but is deeper than in the Chinese or African specimens. A linear tubercle is also present but not enlarged as in the more robust Ngandong crania (1, 6, 10, 11, 12); it is similar to those shown by Ngandong 7 and Sm 1. This tubercle is absent or slight in ZKD 11 and 12, Sangiran 2 and 17, and the African specimens. Of the two "archaic" specimens, Kabwe shows a thinner torus with a relatively strong concavity demarcating the superior toral margin, while Petralona shows no clear separation of the torus from the occipital squama. In Petralona, where the occipital bone is preserved in its full extent, the torus does not project strongly away from the squama. In both specimens, the nuchal surface shows distinct but relatively shallow muscular fossae, and in Petralona a small external occipital crest is preserved. The Sm 3 occipital torus is most similar to, but less developed than, that of Ngandong 7. It is much more gracile than the heavily constructed tori of the ZKD and the Ngandong 6 and 12 specimens.

The left margin of the foramen magnum is completely broken away in Sm 3, but the posterior part of the right lateral border is preserved although eroded and damaged. There appears to be a well-developed bony bulge along the preserved posterolateral border, probably representing a postcondyloid tuberosity as described by Weidenreich (1951). These bony swellings flank the posterolateral wall of the foramen magnum, originating behind the occipital condyles and separated from them by a narrow groove, as seen in Ngandong 7 (Fig. 8). According to Weidenreich (1951, p. 264–265), the Ngandong fossils are distinctive in the strong expression of this trait. He also noted that a postcondyloid tuberosity is present, although partially

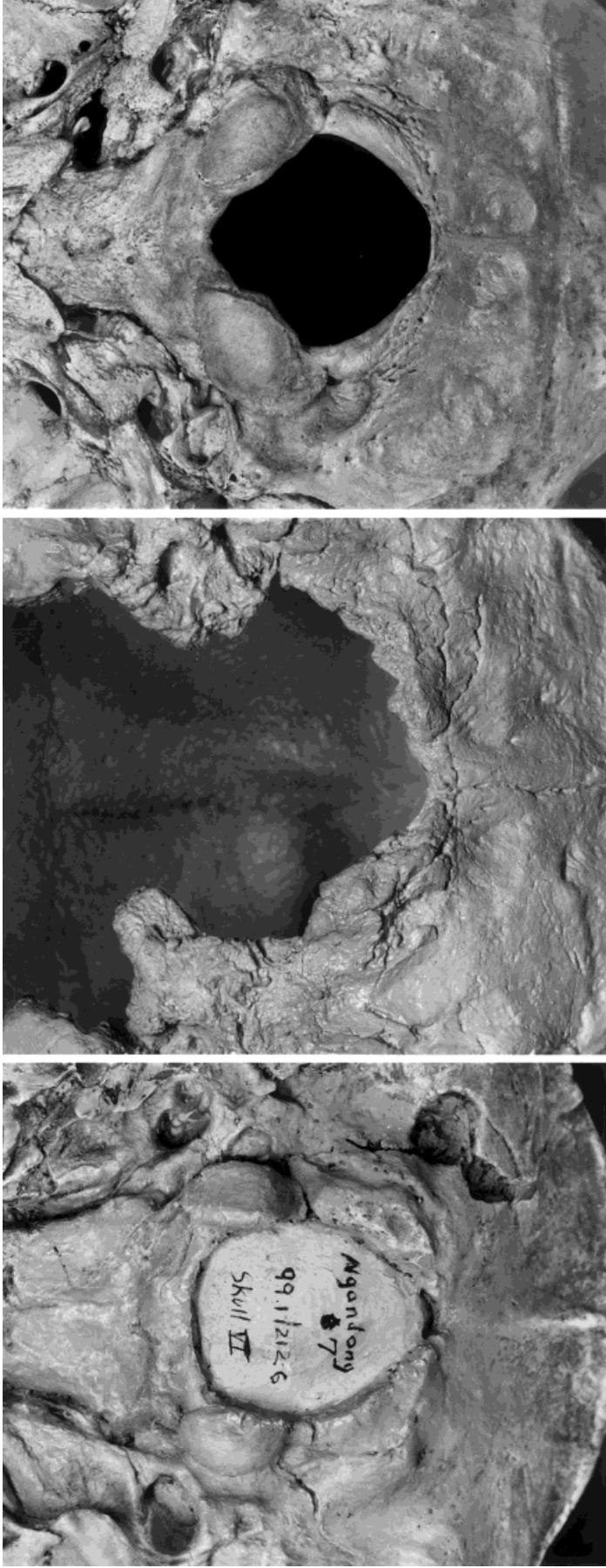


Fig. 8. Basal view of the foramen magnum in (left to right) Ngandong 7 (cast), Sm 3 cast, and modern Tasmanian. Note the presence in Ngandong 7 of postcondyloid tuberosities behind the occipital condyles and an opisthionic recess (narrowing) at the rear of the foramen magnum; these features are also suggested in Sm 3, despite breakage, while the modern cranium has a semi-circular foramen with only a slight swelling of the margin behind the condyles.

broken off, in Zhoukoudian 12, and that slight tuberosities can be found in some modern human populations, particularly Australian and Tasmanian aborigines. Weidenreich (1951) reported, and Rightmire (1993) confirmed, that postcondyloid tuberosities are indeed preserved in Ngandong 1, 7, and 12. Ngandong 11 and possibly 10 also exhibit this feature. Sangiran 4 and 17, ZKD 11, and ER 3733 and 3883 lack any evidence of it; WT 15000 shows some ridging in this area, as stated also by Walker and Leakey (1993), but does not present a true tuberosity. The well-developed postcondyloid tuberosity in Sm 3 is similar to those in the Ngandong sample.

Approaching the posterior end of the postcondyloid tuberosity, the foramen magnum narrows and elongates near opisthion, a characteristic that Weidenreich (1951) described as a "recess." This "opisthionic recess" refers to the narrow portion of the foramen magnum that begins just posterior to the postcondyloid tuberosities and ends at opisthion, as opposed to the nearly semicircular shape of the rear of the foramen magnum in modern humans (Fig. 8). There is a marked expression of this recess in Ngandong 1, 7, and 12. The African specimens ER 3733 and 3883 exhibit a relatively ovate foramen magnum with no narrowing at the opisthion region, as do the two most complete crania from Zhoukoudian (ZKD 11 and 12). Sangiran 4 exhibits an oval foramen magnum that lacks an opisthionic recess, while Sangiran 17 shows some narrowing of the opisthionic region, but far less than in the Ngandong crania. Assessment of this feature in Sm 3 is ambiguous due to lack of preservation of the region. However, the posterolateral rim of the foramen magnum reveals a minor posterior extension at opisthion suggesting that an opisthionic recess was present in Sm 3.

DISCUSSION

The Sm 3 fossil calvaria from Indonesia has been analyzed by geometric morphometrics and comparative morphology. The comparative sample included 10 modern human crania from Tasmania and North China, as well as casts of 18 crania usually identified as *Homo erectus* (only 11 were used in the morphometric study) and two others often termed "archaic *Homo sapiens*" (see Table 1). Detailed morphological description of Sm 3 is provided by Márquez et al. (2001) while Broadfield et al. (2001) discuss its paleoneurology. The major questions posed during this study were: 1.) to which of the three *Homo* taxa studied is Sm 3 most comparable? 2.) does Sm 3 fall in any way intermediate between *Homo erectus* and modern *Homo sapiens*? 3.) can the sex of Sm 3 be determined? and 4.) does the method of geometric morphometrics provide information not readily available from classical comparative morphology?

Affinities of Sm 3

Geometric morphometric analysis involved the collection of 3D coordinates of five midsagittal landmarks and a series of points between them. After conversion to 2D coordinates, the inter-landmark points were resampled to yield "lines" consisting of 50 semi-landmarks on each specimen; landmarks and lines were analyzed separately. The lines provided much greater detail given the higher number of coordinates, but the two analyses yielded basically similar results. The modern human specimens were clearly separated from the known fossils in a graphical

superimposition based on Procrustes fitting of semi-landmarks as well as in both a principal components (PCA) of the aligned Procrustes coordinates and a canonical discriminant (CDA) analysis of the PCA scores. The two "archaic *Homo sapiens*" specimens are not clearly distinguishable in either analysis from the *Homo erectus* range in the sagittal profile. Sm 3 fell between the fossil and modern groups in the Procrustes aligned image (Fig. 2) and also in the PCA (Fig. 3) and CDA (Fig. 4), where it was closer to the fossils, and especially to those from Ngandong in the CDA. When treated as an unknown in the DA, Sm 3 was classified as *H. erectus*, while two of the known *H. erectus* were misclassified as "archaic *H. sapiens*". When the DA was applied to landmark data, Sm 3 was classified as "archaic *H. sapiens*", along with three of the *H. erectus*. A minimum spanning tree derived from the semi-landmark Procrustes distances (Fig. 5) placed Sm 3 between the two fossil groups, distant from the modern humans. A permutation test on these distances (Table 3) suggested that Sm 3 (and also *H. erectus*) could potentially be included with the "archaic *H. sapiens*" sample, but when a Bonferroni correction is applied, the distance between Sm 3 and *H. erectus* falls below significance; thus, the three fossil groups are not statistically distinguishable by this test. In sum, Sm 3 falls within the range of variation of the studied *Homo erectus* sample (see Fig. 2b), which is not readily distinguishable from "archaic *H. sapiens*". On the other hand, it is the individual most similar in shape to anatomically modern humans, especially in the frontal region, in its sagittal profile.

The comparative morphological analysis involved visual comparison of casts, with reference to various cited publications. Again, Sm 3 is most similar overall to Indonesian representatives of *Homo erectus*, especially those from Ngandong and Sambungmacan.

In frontal bone morphology, the supraorbital torus is gracile and most similar to those of female specimens, such as Ngandong 7. The midline supratoral plane is steeper vertically and glabella projects less anteriorly in Sm 3 than in any of the other *H. erectus* fossils examined here. The supratoral region of Sm 3 is most similar to the Ngandong specimens in that it shows no sulcus and its plane is straight above glabella but concave above the trigones. The postorbital constriction of Sm 3 (see Fig. 6) is closest to that of Indonesian fossils: Ngandong, Sm 1, and Ngawi. The upper portion of the frontal squama in Sm 3 is more rounded than in the Indonesian and most African (or European) fossils examined, but it is similar to those from Zhoukoudian and to ER 3733. Although these latter specimens are superficially similar to Sm 3 in this respect, they show a much stronger frontal keeling which greatly contributes to the rounded shape of their frontal squama in lateral view. The pattern of sagittal keeling on the frontal and anterior parietal in Sm 3 is distinctive: weak on the frontal but stronger on the parietal, without effect on the frontal squama rounding, and no bregmatic eminence or coronal ridging. This is most similar to Sm 1, less so to Sangiran 2 and 17.

Although an angular torus has long been considered a characteristic of *Homo erectus*, none is visible on Sm 3, which instead presents only a slight swelling. In fact, the occurrence of the torus is variable in several studied samples: Sangiran, Ngandong, Zhoukoudian, East Africa, and Sambungmacan. The tympanomastoid fissure between the mastoid process and the tympanic, another feature

typical of Asian *H. erectus*, is well developed in Sm 3 and most similar to those from Ngandong (see Fig. 7). Other Asian fossils present a weaker fissure with a different shape, while most of the African specimens lack it. The presence of a Ngandong-like fissure in WT 15000 may oppose the distinction between African and Asian populations based on this feature (or may be age-related). The squamotympanic fissure in Sm 3 runs in the deepest portion of the deep and antero-posteriorly short mandibular fossa, as in all other Indonesian fossils and OH 9.

The supramastoid crest of Sm 3 courses upward at an angle to the suprameatal crest to cross the squamosal suture above the parietal incisure. It is separated completely from the mastoid crest by a wide and shallow supramastoid sulcus. This pattern is matched in the Ngandong fossils and in Sm 1 and Sgr 4, but differs in Zhoukoudian, Sgr 2 and 17, the African specimens, and “archaic *Homo sapiens*”. On the other hand, the prominence of the suprameatal and supramastoid crests in Sm 3 is most similar to that of Zhoukoudian, Sangiran 17, and Sm 1. The crests are weak in the African specimens (including Kabwe), while Ngandong is variable in this feature.

The occipital torus of Sm 3 is rather robust and thick supero-inferiorly, much as in Ngandong 7. The superior margin of the central region is arched as in Sm 1 and the Ngandong series, rather than straight as seen in most other *H. erectus* fossils. The nuchal scale in Sm 3 is moderately excavated for muscular attachment, and an external occipital crest is visible. This region is less well developed than in the Ngandong series or Sm 1, but more so than in the Sangiran, Zhoukoudian, or African fossils. The greatest similarity of Sm 3 in the occipital torus area is to Sm 1 and Ngandong 7, although the angle between its nuchal and occipital scales is less acute than in any of the fossils observed. In the region of the foramen magnum (see Fig. 8), Sm 3 appears to present both a postcondyloid tuberosity and an opisthionic recess, although breakage renders these observations questionable. The preserved morphology is closest to that seen in the Ngandong sample.

In sum, both the geometric morphometric, and comparative morphological analyses link Sm 3 most closely with the Ngandong sample and Sm 1, with other Indonesian fossils such as Trinil 2 and those from Sangiran also being generally similar. The Zhoukoudian sample and the several African *Homo erectus* examined were usually different morphologically from Sm 3, although ZKD and ER 3733 showed similarity to it in the curvature of the upper frontal scale. Both “archaic *Homo sapiens*” fossils examined and the two samples of modern humans differed consistently from Sm 3 and (except in the sagittal profile morphometrics) from most *H. erectus* fossils. In two areas, Sm 3 was quite distinctive among all the fossils studied. On the lower frontal, the supratral plane is more vertical and the glabella more anteriorly projecting than any fossil, although it did not closely approach the shape seen in modern humans. The occipital angle is less acute than in the fossils examined.

Overall, there would appear to be no strong reason not to include Sm 3 as a member of *Homo erectus*, especially when that taxon is broadly interpreted to include African representatives. It is morphologically distinctive in the lower frontal and mid-occipital regions but in general falls well within the range of variation of *Homo erectus* in both analyses. Those distinctions, however, are broadly “in the

direction” of modern humans in that they represent an “unrolling” of the neurocranium both anteriorly and posteriorly. In the geometric morphometric visualizations, Sm 3 was consistently placed between the other fossils and modern humans as well. What is the evolutionary meaning of this intermediacy?

Currently, there are two major models of the origin of modern humans: regional continuity and single-region dispersal (see, e.g., Tattersall and Delson, 2000; Stringer, 2000; Thorne, 2000). The former envisions *H. erectus* (termed early *H. sapiens* by its leading proponents) as evolving into modern *H. sapiens* in various Old World regions in parallel, with migrational gene flow serving to link all populations at any given time. Under such a model, the apparently more modern morphology of Sm 3 among known Indonesian *H. erectus* might be interpreted as documenting such in situ evolution. But there is no evidence that the morphology of Sm 3 was typical of the biological population of which it was part; it might have been just a variant individual which (perhaps in part as a result of small body size) shared superficial similarity with later humans. Paleontologists must usually assume that any unique individual discovered was representative of the biological population in which it lived, but with the recovery of additional specimens (e.g., OH 5 is probably an extreme member of the taxon to which it belongs as holotype), this is sometimes later shown to be untrue. The geographically closest individual, Sm 1, shared a number of features with Sm 3, but certainly not its most distinctive aspects. In fact, there is no way at present to choose among these three possible scenarios: 1.) Sm 3 was a representative of a population of *H. erectus* evolving in the direction of modern humans; 2.) Sm 3 was a representative of a morphologically distinctive population of Indonesian *H. erectus* which later merged with more “typical” forms or died out, not leading to any specific later group—most of the authors prefer this alternative—or 3.) Sm 3 was a distinctive individual among “typical” Indonesian *H. erectus*. Further specimens from the Sambungmacan area might resolve this uncertainty, but only if they share the novel features of Sm 3.

Sex Determination

As noted by Márquez et al. (2001), among many others, has noted, the identification of sex in human fossils is a probabilistic activity. Features such as relative robusticity can only be safely utilized when a sample is available within which relativity can be assessed. Here, one is dealing with a single individual specimen which has been referred to a taxon characterized by a higher overall degree of robusticity than in modern humans, which renders the uncertainty even greater. Nonetheless, there is a broad consistency of admittedly weak indicators which point to Sm 3 having been a female.

In the geometric morphometrics, the centroid size (CS) of Sm 3 is the smallest of any fossil, falling between the smallest modern human and ER 3733 (generally viewed as female). In the principal component analysis (PCA) of the semi-landmarks, ANOVAs revealed a marginally significant sex effect for PC1 and a more significant one for PC4; the position of Sm 3 appears weakly to suggest a female identification. In terms of morphology, the gracility of its supraorbital torus and of its sagittal and coronal ridging also seem to indicate female sex. The lack of an angular torus in Sm 3 is another potential indicator of

female sex, but as noted above, the putatively female ZKD 11 has a stronger torus than the supposed male ZKD 12. On the other hand, the strong supramastoid crest in Sm 3 would be expected in a male rather than female individual. Moreover, Santa Luca (1980) has discussed how *Homo erectus* "females" (as estimated from overall size) seem to present more keeling but less development of other "superstructures" (angular, occipital, and supraorbital tori; supramastoid and other crests) than males. The mosaic seen in Sm 3, of relatively gracile to nonexistent tori and circum-bregmatic ridging, combined with small size, does not correspond to either pattern observed by Santa Luca, but that may only reflect the situation in Ngandong. Given the patterns of sexual dimorphism represented by the Ngandong sample (male 12 and 6 vs. female 7 and 1), Sangiran (male 17 and 4 vs. female 2), Zhoukoudian (male 12 vs. female 11), and East Africa (male OH 9 [and WT 15000] vs. female ER 3733 and 3883), the Sumbungmacan fossils could also represent a dimorphic duo.

Contributions of Geometric Morphometrics

As has been discussed by many authors (e.g., Rohlf and Marcus, 1993), geometric morphometrics is "superior" to traditional or inter-landmark morphometrics in that it preserves the interrelationships of all landmarks and the surfaces between them. This study is one of the first (in paleoanthropology at least) to analyze coordinates from lines connecting several landmarks (see also Bookstein et al., 1999; Dean et al., 1996) and the first to apply these methods to determine the affinities of a newly recovered fossil hominin. The several statistical tests applied here represent some of the ways in which geometric morphometric data can be examined to yield phenetic estimates of the evolutionary relationships (and sex) of individuals, samples, and taxa. The intermediate position of Sm 3 indicated by the graphical superimposition as well as the multivariate techniques is not clearly revealed by the comparative morphological examination of the same specimen or specimens. Indeed, both the distinctive frontal elevation and the more "open" occipital angle were observed in the graphical Procrustes analysis before being confirmed by the morphological study. One weakness of this morphometric work is its confinement to the 2D analysis of features in the sagittal plane, but that limitation will be exceeded through continued advances in this field. Our research group is also seeking ways to combine these continuous-variable methods with the coded discontinuous approach required for numerical cladistic analysis (see also, e.g., Naylor, 1996; Thiele, 1993; Zeitoun, 2000).

An unexpected result of this geometric morphometric analysis is the finding that the Procrustes-aligned profiles of modern and extinct samples crossed near lambda and (less clearly) bregma, which might imply that the growing margins of the parietal (and other bones?) constrain the location of evolutionary change in cranial shape. This type of graphical observation could not have been discerned using other forms of analysis.

ACKNOWLEDGMENTS

We thank Henry Galiano for his generosity in permitting us access to the Sm 3 calvaria while it was in his possession and for his honorable action in returning it to the Indonesian authorities. We thank Drs. Ian Tattersall

and Jeffrey Laitman for assistance during the preparation of this manuscript and Drs. Susan Antón, Martin Friess, and Philip Rightmire for comments on an earlier draft. Figures 1, 7, and 8 were produced by Lorraine Meeker and Chester Tarka with expertise we have come to expect. This is NYCEP morphometrics contribution number 2.

LITERATURE CITED

- Andrews P. 1984. On the characters that define *Homo erectus*. *Courier Forschungsinstitut Senckenberg* 69:167–175.
- Ascenzi A, Bidditu I, Cassoli PF, Segre AG, Segre-Naldini E. 1996. A calvarium of late *Homo erectus* from Ceprano, Italy. *J Human Evol* 31:409–423.
- Baba H, Aziz F, Watanabe N. 1990. Morphology of the fossil hominid tibia from Sumbungmacan, Java. *Bull Nat Sci Mus Tokyo, ser D (Anth)* 16:9–18.
- Boedihartono. 1998. A new *Homo erectus* finding. *Antropologi* 54: 121–125.
- Bookstein FL. 1996. Combining the tools of geometric morphometrics. In: Marcus LF, Corti M, Loy A, Naylor GJP, Slice DE, editors. *Advances in morphometrics*. New York: Plenum. p. 131–151.
- Bookstein FL. 1997. Landmark methods for forms without landmarks: morphometrics of group differences in outline shape. *Med Image Anal* 3:225–43.
- Bookstein FL. 1998. A hundred years of morphometrics. *Acta Zool Acad Scientiarum Hungaricae* 44:7–59.
- Bookstein FL, Green WDK. 1994. Edgewarp: a flexible program package for biometric image warping in two dimensions. *Proc SPIE* 2359:135–147.
- Bookstein FL, Schafer K, Prossinger H, et al. 1999. Comparing frontal cranial profiles in archaic and modern homo by morphometric analysis. *Anat Rec* 6:217–224.
- Broadfield DC, Holloway RL, Mowbray K, Silvers A, Yuan MS, Márquez S. 2001. Endocast of Sumbungmacan 3 (Sm 3): A new *Homo erectus* from Indonesia. *Anat Rec* 262:369–379.
- Dean D. 1993. The Middle Pleistocene *Homo erectus/H. sapiens* transition: new evidence from space curve statistics. Ph.D. diss., City University of New York.
- Dean D, Marcus LF, Bookstein F. 1996. Chi-square test of biological space curve affinities. In: Marcus LF, Corti M, Loy A, Naylor GJP, Slice DE, editors. *Advances in morphometrics*. New York: Plenum, p. 235–251.
- Howells WW. 1973. Cranial variation in man: a study by multivariate analysis of patterns of difference among recent human populations. *Peabody Mus Pap* 67:1–259.
- Jacob T. 1975. Morphology and paleoecology of early man in Java. In: Tuttle R, editor. *Paleoanthropology: morphology and paleoecology*. The Hague: Mouton. p. 311–325.
- Jacob T. 1976. Solo man and Peking man. In: Sigmon BA, Cybulski JS, editors. *Papers in honor of Davidson Black*. Toronto: University of Toronto Press. p. 87–104.
- Jacob T. 1999. The two Sumbungmacan skull caps (Sm 1 and Sm 3). Beijing: Zhoukoudian Symposium.
- Jacob T, Soejono RP, Freeman LG, Brown FH. 1978. Stone tools from mid-Pleistocene sediments in Java. *Science* 202:885–887.
- Macintosh NWG, Larnach SL. 1972. The persistence of *Homo erectus* traits in Australian Aboriginal crania. *Arch Phys Anthropol Oceania* 7:1–7.
- Marcus LF, Frost SR, Delson E. 1997. Comparison of Polhemus 3Draw Pro and Microscribe 3DX. "Internet-publication," posted to: Biological Morphometrics Mailing List Archived at <http://research.amnh.org/nycep/manuscripts.html>
- Marquez S, Mowbray K, Sawyer GJ, Jacob T, Silvers A. 2000. A new fossil hominin calvaria from Indonesia—Sumbungmacan 3. *Anat Rec* 262:344–368.
- Matsu'ura S, Kondo M, Aziz F, Sudijono, Narasaki S, Watanabe N. 2000. First known tibia of an early Javanese hominid. *Curr Anth* 41:297–300.
- Naylor GJP. 1996. Can partial warp scores be used as cladistic characters? In: Marcus LF, Corti M, Loy A, Naylor GJP, Slice DE,

- editors. *Advances in morphometrics*. New York: Plenum. p. 519–530.
- Rice WR. 1989. Analyzing tables of statistical tests. *Evolution* 43:223–225.
- Rightmire GP. 1993. *The evolution of Homo erectus*, comparative anatomical studies of an extinct human species. New York: Cambridge University Press.
- Rohlf FJ. 1998a. tpsRegr: shape regression. 1.13 ed. Stony Brook, NY: Department of Ecology and Evolution, State University of New York at Stony Brook.
- Rohlf FJ. 1998b. tpsRelw: analysis of relative warps. 1.15 ed. Stony Brook, NY: Department of Ecology and Evolution, State University of New York at Stony Brook.
- Rohlf FJ. 2000. Statistical power comparisons among alternative morphometric methods. *Am J Phys Anthropol* 111:463–478.
- Rohlf FJ, Marcus LF. 1993. A revolution in morphometrics. *Trends Ecol Evol* 8:129–132.
- Rohlf FJ, Slice DE. 1990. Extensions of the Procrustes method for the optimal superimposition of landmarks. *Syst Zool* 39:40–59.
- Santa Luca AP. 1980. The Ngandong fossil hominids: a comparative study of a far eastern *Homo erectus* group. *Yale University Pubs Anthro* 78:1–75.
- Sartono S. 1990. A new *Homo erectus* skull from Ngawi, east Java. *Indo-Pacific Prehistory Assn Bull* 11:14–22.
- SAS Institute Inc. 1989. SAS/STAT user's guide, ver. 6, 4th ed., vol. 1. SAS Institute, Inc.: Cary, NC.
- Slice DE. 1993. Extensions, comparisons, and applications of superimposition methods for morphometric analysis. Ph. D. diss, State University of New York at Stony Brook.
- Stringer CB. 1984. The definition of *Homo erectus* and the existence of the species in Africa and Europe. *Courier Forschungsinstitut Senckenberg* 69:131–143.
- Stringer CB. 2000. Modern human origins: out of Africa. In: Delson E, Tattersall I, Van Couvering JA, Brooks AS, editors. *Encyclopedia of human evolution and prehistory*, 2nd ed. New York: Garland. p. 429–432.
- Stringer CB, Howell FC, Melentis JK. 1979. The significance of the fossil hominid skull from Petralona, Greece. *J Archaeol Sci* 6:235–253.
- Tattersall I, Delson E. 2000. Modern human origins: introduction. In: Delson E, Tattersall I, Van Couvering JA, Brooks AS, editors. *Encyclopedia of human evolution and prehistory*, 2nd ed. New York: Garland. p. 425–427.
- Thiele K. 1993. The holy grail of the perfect character: the cladistic treatment of morphometric data. *Cladistics* 9:275–304.
- Thorne A. 2000. Modern human origins: multiregional evolution. In: Delson E, Tattersall I, Van Couvering JA, Brooks AS, editors. *Encyclopedia of human evolution and prehistory*, 2nd ed. New York: Garland. p. 425–429.
- Walker AC, Leakey R, eds. 1993. *The Nariokotome Homo erectus skeleton*. Cambridge: Harvard University Press.
- Weidenreich F. 1943. The skull of *Sinanthropus pekinensis*: a comparative study on a primitive hominid skull. *Palaeontol Sin Ser D* 10:1–298.
- Weidenreich F. 1951. Morphology of Solo man. *Am Mus Nat Hist, Anthropol Pap* 43:207–290.
- White TD. 2000. *Human osteology*, 2nd ed. San Diego: Academic.
- Wood B. 1984. The origins of *Homo erectus*. *Courier Forschungsinstitut Senckenberg* 69:99–111.
- Wood B. 1991. Koobi Fora research project volume 4, hominid cranial remains. Oxford: Clarendon Press.
- Zeitoun V. 2000. Utilisation des données continues en cladistique—un exemple paléanthropologique: *Homo erectus*. *Biom Hum Anthropol* 17:139–145.